JOURNAL OF AGRICULTURAL AND FOOD CHEMISTRY

Article

pubs.acs.org/JAFC

Monascuspiloin Induces Apoptosis and Autophagic Cell Death in Human Prostate Cancer Cells via the Akt and AMPK Signaling Pathways

Rong-Jane Chen,[†] Chin-Ming Hung,[†] Yen-Lin Chen,[‡] Ming-Der Wu,[‡] Gwo-Fang Yuan,[‡] and Ying-Jan Wang*,[†]

[†]Department of Environmental and Occupational Health, National Cheng Kung University Medical College, Tainan 70428, Taiwan

[‡]Bioresource Collection and Research Center (BCRC), Food Industry Research and Development Institute, Hsinchu 30099, Taiwan

ABSTRACT: *Monascus* pigments have been reported to possess anticancer effects in various cancer cells; however, the molecular mechanisms of their anticancer properties remain largely unknown. Monascuspiloin is an analogue of the *Monascus* pigment monascin, and its anticancer growth activity against human prostate cancer cells was evaluated using *in vitro* and *in vivo* models. Monascuspiloin effectively inhibits the growth of both androgen-dependent LNCaP and androgen-independent PC-3 human prostate cancer cells. Monascuspiloin preferentially induces apoptosis in LNCaP cells by attenuating the PI3K/Akt/mTOR pathway. In androgen-independent PC-3 cells, monascuspiloin induces G2/M arrest and autophagic cell death by an AMPK-dependent pathway. Induction of autophagy in PC-3 cells further sensitizes cells to apoptosis induced by monascuspiloin. Monascuspiloin inhibits tumor growth in nude mice bearing PC-3 xenografts through induction of apoptosis and autophagy. This study is the first to demonstrate that monascuspiloin has therapeutic potential for the treatment of both androgen-dependent and -independent human prostate cancers.

KEYWORDS: *Monascuspiloin, apoptosis, autophagic cell death, Akt/mTOR, AMPK, prostate cancer*

INTRODUCTION

Red mold rice (RMR) is produced by the fermentation of rice with *Monascus* sp.[1] RMR has been widely used as both a food additive and a traditional pharmaceutic in Asia because of its multifunctional metabolites.[2] These functional metabolites include the following:[3] (a) a group of yellow, orange, and red pigments, (b) a group of antihypercholesterolemic agents, including monacolin K, and hypotensive agents,[4] (c) antioxidant compounds, such as dimerumic acids,[5] and (d) antibacterial compounds, including pigment and citrinin.[6] Recently, it has been reported that RMR and its metabolites possess anticancer activity in many cancers.[7,8] *Monascus* pigments are a series of azaphilone compounds, including yellow pigments (monascin and ankaflavin), orange pigments (monascorubrin and rubropunctatin), and red pigments (monascorubramine and rebropunctamine).[9] These pigments were reported to inhibit tumor promotion in a two-stage carcinogenesis model in mice that was initiated by 7,12-dimethylbenz[*a*]anthracene (DMBA) and promoted by 12-*O*-tetradecanoylphorbol 13-acetate (TPA).[10,11] Additionally, novel azaphilonoid derivatives from RMR have recently been reported to exert anti-inflammatory and anticancer effects on both human laryngeal carcinoma and colon adenocarcinoma cell lines.[12,13] Therefore, it is of value to purify natural anticancer agents from RMR pigments for evaluation of their anticancer activity.

Monascuspiloin (MP), a yellow pigment first isolated from *Monascus* fermented rice by our group, has a structure similar to the well-known *Monascus* pigment, monascin. Monascin has anti-inflammatory and cytotoxic effects.[3] Additionally, Hong et al. reported that *Monascus* pigments were able to inhibit prostate cancer (PCa) cell proliferation and stimulate apoptosis.[14] PCa is the most prevalent cancer in men worldwide. Conventional treatment for prostate cancer includes surgical excision, irradiation, chemotherapy, and androgen deprivation for advanced prostate cancer. However, nearly all patients on androgen deprivation therapy will progress to castration-resistant prostate cancer (CRPC), for which there is no curative treatment.[15] As a result, prostate cancer remains the second-leading cause of cancer-related death in men in the United States.[16] Treatment of CPCR is a challenge for clinicians. Thus, new rational approaches to treat prostate cancer are required.

PCa cells likely require specific metabolic alterations that cooperate with genetic events to induce neoplastic transformation and tumor progression. These alterations are induced by both androgen and PI3K/Akt/mTOR pathways. Current estimates suggest that the PI3K/Akt/mTOR pathway is upregulated in 30−50% of PCa tumors and is associated with increasing tumor stage, grade, and risk of biochemical recurrence. Novel inhibitors targeting this pathway may result in therapeutic benefits for patients with prostate cancer.[17] Additionally, the other approach for PCa therapy is to target a master regulatory switch of major oncogenic and metabolic signaling pathways, such as the 5′-AMP-activated protein kinase (AMPK) pathway. AMPK is an energy-sensing serine/threonine kinase that is activated under conditions of metabolic

Received: April 20, 2012
Revised: June 27, 2012
Accepted: June 27, 2012
Published: June 27, 2012

stress.[18] A recent study suggested that AMPK dysregulation may provide a mechanistic link between metabolic syndrome (MS) and PCa. Therefore, drugs that ameliorate MS conditions through AMPK activation may be beneficial for PCa prevention and treatment.[19]

Activation of AMPK can induce apoptosis through phosphorylation of p53 and p27, inhibit cell growth and protein synthesis through inactivation of mTOR, and promote autophagy.[20] Induction of autophagic cell death may be an ideal approach in cancers with defects in the apoptotic pathway, which is the case in many advanced, drug-resistant, and metastatic cancers.[21] Thus, the PI3K/Akt, AMPK, and autophagy pathways are considered new targets for prostate cancer therapy. Therefore, in this study, we sought to characterize the nature of the cell death induced by MP and its relationship to the PI3K/Akt and AMPK signaling pathways in androgen-dependent and -independent prostate cancer cells.

MATERIALS AND METHODS

Preparation of RMR and Extraction of Monascuspiloin. *Monascus pilosus* M93 was obtained from BCRC, FIRDI (Hsinchu, Taiwan) and maintained on potato dextrose agar (PDA; Difco). The strain was plated onto PDA plates and cultivated at 25 °C for 7 days. Then, the spores were washed out from the PDA plate using sterile water, and the concentration of the spore suspension was adjusted to 1×10^6/mL. After the spores enrichment step, 1 mL of spores suspension was inoculated into 250 mL shake flasks containing 50 mL of RGY medium (which contains 3% rice starch, 7% glycerol, 1.2% polypeptone, 3% soybean powder, 0.1% $MgSO_4$, and 0.2% $NaNO_3$) and cultivated with shaking (150 rpm) at 25 °C for 3 days to obtain the mycelium broth of M93.

For the production of red mold rice (RMR), 50 450 mL glass bottles each containing 75 g of rice and 75 mL of deionized (DI) water were sterilized for 20 min, at 121 °C. For each bottle, M93 mycelium broth (7.5 mL) and RGY medium (7.5 mL) were added and incubated at 25 °C for 21 days (7.5 mL of RGY medium was added per bottle at the 10th day of the incubation) and then lyophilized to remove water. The RMR (1 kg) was extracted with 95% ethanol (3 L) at 25 °C for 24 h, and then ethanol was remove by vacuum drying to obtain the crude extract of RMR. The amounts of monascuspiloin (MP) in crude extracts were measured by high-performance liquid chromatography (HPLC) using a purospher star RP-18 column (Merck), in which the mobile phase consisted of 60% acetonitrile containing 0.1% phosphate at a 1.0 mL/min flow rate. After filtration, the ethanol extract was concentrated and ethyl acetate (EA) was added to obtain an EA-soluble fraction. The EA-soluble fraction was subjected to a silica gel column (70−230 and 230−400 mesh) (Merck), eluting with *n*-hexane/ethyl acetate (2:1). The eluted fraction was concentrated under reduced pressure, followed by purification from preparative thin-layer chromatography (silica gel 60 F-254, Merck) with *n*-hexane/EtOAc (2:1) to obtain MP. MP was analyzed employing a linear gradient from 10 to 90% of acetonitrile in water over 10 min and a flow rate of 1 mL/min, and the purity of the MP compound was verified by means of ^{1}H nuclear magnetic resonance (NMR), high-resolution mass spectrometry (HRMS), and HPLC−ultraviolet (UV) analyses and reached a level >95%.

MP, isolated as a yellowish oil, was assigned the molecular formula $C_{21}H_{28}O_5Na$ by electrospray ionization (ESI)−MS) ($[M + Na]^+$, m/z 383) and HR-ESI−MS ($[M + Na]^+$, m/z 383.1832). MP was similar to that of a known compound, monascin. The structure of MP was determined to be (3*S*,3a*R*,9a*R*)-3a,4-dihydro-3-((*S*)-1-hydroxyhexyl)-9a-methyl-6-((*E*)-prop-1-enyl)-3*H*-furo[3,2-*g*]isochromene-2,9-(8*H*,9a*H*)-dione (Figure 1A).

Cell Culture and Chemicals. The human prostate cancer cell lines LNCaP [androgen-dependent, American Type Culture Collection (ATCC) number CRL-1740] and PC-3 (androgen-independent, ATCC number CRL-1435) were purchased from Biosource Collection and Research Center (BCRC, Hsinchu, Taiwan) (ATCC, Manassas, VA). Both cells lines were maintained in RPMI 1640 medium (Sigma-Aldrich Co., St. Louis, MO) supplemented with 100 units/mL penicillin, 100 μg/mL streptomycin (Life Technologies, Inc., Gaithersburg, MD), and 10% heat-inactivated fetal calf serum (HyClone, South Logan, UT). 3-Methyladenine (3-MA) was purchased from Sigma-Aldrich, Co. PI3K inhibitor LY294002 was obtained from Cell Signaling (Beverly, MA). Acridine orange (AO) was purchased from USB cooperation (Cleveland, OH). Z-VAD-FMK was obtained from R&D Systems, Inc. (Minneapolis, MN). Antibodies against cyclin B, phospho-cdc-2, cdc-2, Bcl-2, Bax, Bad, Bcl-xl, Beclin 1, Akt, phospho-Akt, AMPK, phospho-AMPK, phospho-p70S6K, mTOR, phospho-mTOR, and GAPDH and horseradish peroxidase (HRP)-conjugated anti-mouse and anti-rabbit secondary antibodies were purchased from Cell Signaling. Anti-LC3 antibody was obtained from MBL (Woburn, MA). p70S6K antibody was purchased from BD Biosciences (Franklin Lakes, NJ). Cleaved caspase 3 antibodies were purchased from Epitomics, Inc. (Burlingame, CA). Atg5 antibody was purchased from ABGENT (San Diego, CA).

Cell Viability and Apoptosis Assays. Cells viability, Annexin V staining assay, and DNA laddering methods were performed according to the methods described previously.[22]

Cell Cycle Analyses. Cells were washed, trypsinized, and fixed with 75% ethanol for at least 4 h. After fixation, cells were washed and then stained with 4 μg/mL propidium iodide (PI) for 30 min and then measured by flow cytometry with a FACScan (Becton Dickinson, San Jose, CA).

Detection and Quantification of Acidic Vesicular Organelles with AO Staining. Cells were stained with 1 μg/mL AO for 15 min and analyzed using a fluorescence microscope (Axioscop) equipped with a mercury 100 W lamp, 490 nm band-pass blue excitation filters, a 500 nm dichroic mirror, and a 515 nm long-pass barrier filter. The percentages of acridine vesicular organelles (AVOs) were also analyzed by flow cytometry.

Electron Microscopy. PC-3 cells were treated with MP for 48 h and then fixed with a solution containing 2.5% glutaraldehyde and 2% paraformaldehyde (in 0.1 M cacodylate buffer at pH 7.3) for 1 h. The cells were then post-fixed in 1% OsO_4 in the same buffer for 30 min. Ultrathin sections were observed under a transmission electron microscope (JEOL JEM-1200EX, Japan) at 100 kV.

Western Blot Analyses. Isolation of total cellular lysates, gel electrophoresis, and immunoblotting were performed according to the methods described previously.[22] Immunoreactive proteins were visualized with an chemiluminescent detection system (PerkinElmer Life Science, Inc., Waltham, MA) and BioMax LightFilm (Eastman Kodak Co., New Haven, CT) according to the instructions of the manufacturers.

RNA Interference (RNAi). Arrest-In Transfection Reagent (Thermo Fisher Scientific, Huntsville, AL) was used to transfect cells. RNAi reagents were obtained from the National RNAi Core Facility located at the Institute of Molecular Biology/Genomic Research Center, Academia Sinica, which is supported by the National Research Program for Genomic Medicine Grants of National Science Council (NSC) (NSC 97-3112-B-001-016). The human library is referred to as TRC-Hs 1.0. Individual clones are identified as shRNA TRCN000072178 and shRNA TRCN0000000861.

BALB/C-nu/nu Mouse Xenograft Study. A total of 15 male BALB/C-nu/nu mice, aged 5 weeks, were purchased from the National Laboratory Animal Center (Taipei, Taiwan). They were housed 5 mice per cage in a pathogen-free environment. After acclimation, PC-3 cells (2×10^6 cells) in 0.1 mL 1× phosphate-buffered saline (PBS) were transplanted subcutaneously between the scapulae of each mouse. Once the tumor reached a volume of 80 mm^3, animals were divided into three groups and received intraperitoneal injections of one of the follow items: (1) control (corn oil), (2) 40 mg/kg of MP, and (3) 120 mg/kg of MP, 3 times weekly for a total of six injections. At the end of the experiment, mice were sacrificed and tumor volumes, tumor weights, tumor volume quadrupling times, and tumor growth delay times were calculated to compare the treatment efficacy among each group. Tumor tissues were dissected and used for

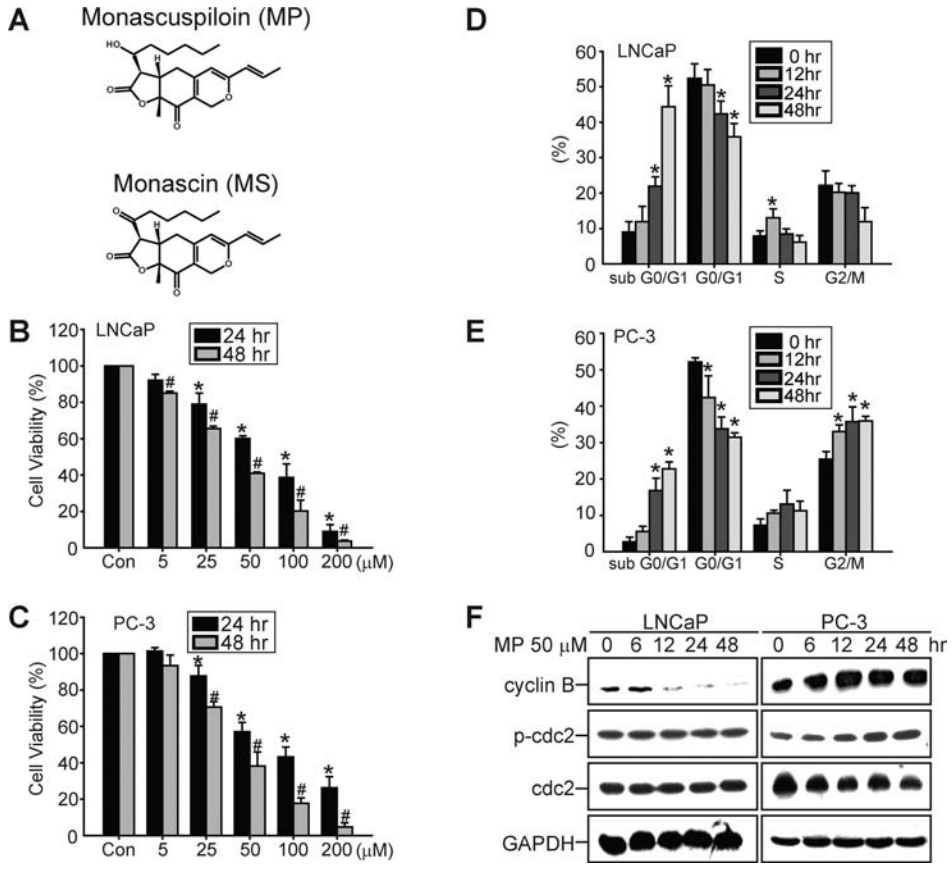

Figure 1. MP treatment inhibits cell viability of PCa cell lines. (A) Chemical structure of monascuspiloin (MP) and monascin (MS). MP inhibits cell viability of (B) LNCaP and (C) PC-3 cells in a concentration-dependent manner at 24 and 48 h. (∗) $p < 0.05$ compared to the control group at 24 h. (#) $p < 0.05$ compared to the control group at 48 h. Mean ± standard error of the mean (SEM); $n = 3$. Cell cycle analysis was performed using flow cytometry in (D) LNCaP and (E) PC-3 cells treated with 50 μM MP in a time-dependent manner. Mean ± SEM; $n = 3$. (∗) $p < 0.05$ compared to the 0 h group. (F) LNCaP (left panel) and PC-3 (right panel) cells were treated with 50 μM MP for indicated times, and then cell lysates were isolated and immunoblotted with anticyclin B, p-cdc-2, and cdc-2 antibodies. Membranes were probed with an anti-GAPDH antibody to confirm equal loading of proteins. Representative data from one of three independent experiments are shown.

immunohistochemistry and immunoblotting analyses to detect expression of caspase 3, PCNA, LC3, Atg12, Atg5, and Beclin 1.

Statistical Analyses. Results are expressed as the mean ± SEM. Experimental data were analyzed using Student's t test. Differences were considered to be statistically significant when the p value was less than 0.05.

RESULTS

Monascuspiloin Inhibits Growth of Prostate Cancer Cell Lines. Figure 1A showed the structure of the *Monascus*-specific pigment monascuspiloin (MP) and its analogue monascin (MS) (Figure 1A). MP was tested for anticancer growth effects on androgen-dependent LNCaP cells and androgen-independent PC-3 prostate cancer cells. MP significantly decreased the growth of both cell lines in a concentration- and time-dependent manner (panels B and C of Figure 1). The IC_{50} values after 48 h of MP treatment are 44.97 ± 2.12 and 46.96 ± 0.95 μM in LNCaP and PC-3 cells, respectively. These results indicate that both androgen-dependent and -independent prostate cancer cell lines possess similar sensitivity to MP treatment. To determine the anticancer growth effects of MP in both cell lines, we analyzed the cell cycle distribution, apoptosis, and autophagy. We found that treatment with 50 μM MP for 24 and 48 h induced a marked increase in LNCaP cells in the sub-G0/G1 phase and concomitantly deceased in the G0/G1 and G2/M phases (Figure 1D). In PC-3 cells, MP only mildly increased the percentage of sub-G0/G1 but significantly induced G2/M arrest in PC-3 cells (Figure 1E). The results of western blot analysis showed that cyclin B and phospho-cdc2 expression increased time-dependently in PC-3 cells treated with MP, further confirming that MP induces G2/M arrest in PC-3 cells but not in LNCaP cells (Figure 1F).

Monascuspiloin Induces Apoptosis in Prostate Cancer Cell Lines. The nature of MP-induced cell death was then analyzed using several markers of apoptosis. Apoptosis was confirmed by DNA laddering (Figure 2A), increased Annexin V staining (Figure 2B), increased cleavage of caspase 3, increased Bax and Bad expression, and decreased Bcl-2 and Bcl-xl expression (Figure 2C) in LNCaP cells after MP treatment in a concentration- and time-dependent manner. The same dosage of MP also slightly increased apoptosis in PC-3 cells (panels A–C of Figure 2). However, the expression of Bax, Bad, and Bcl-xl in PC-3 cells did not show remarkable changes following MP treatment when compared to LNCaP cells (Figure 2C). These results indicate that MP treatment preferentially induces apoptosis in androgen-dependent LNCaP cells. Next, we used the pan-caspase inhibitor to confirm that the anticancer effects of MP contributed to the induction of apoptosis. Pretreatment with the pan-caspase inhibitor (20 μM) reduced MP-induced apoptosis and partially restored cell viability in LNCaP cells (panels D and E of Figure 2). However, cell viability did not

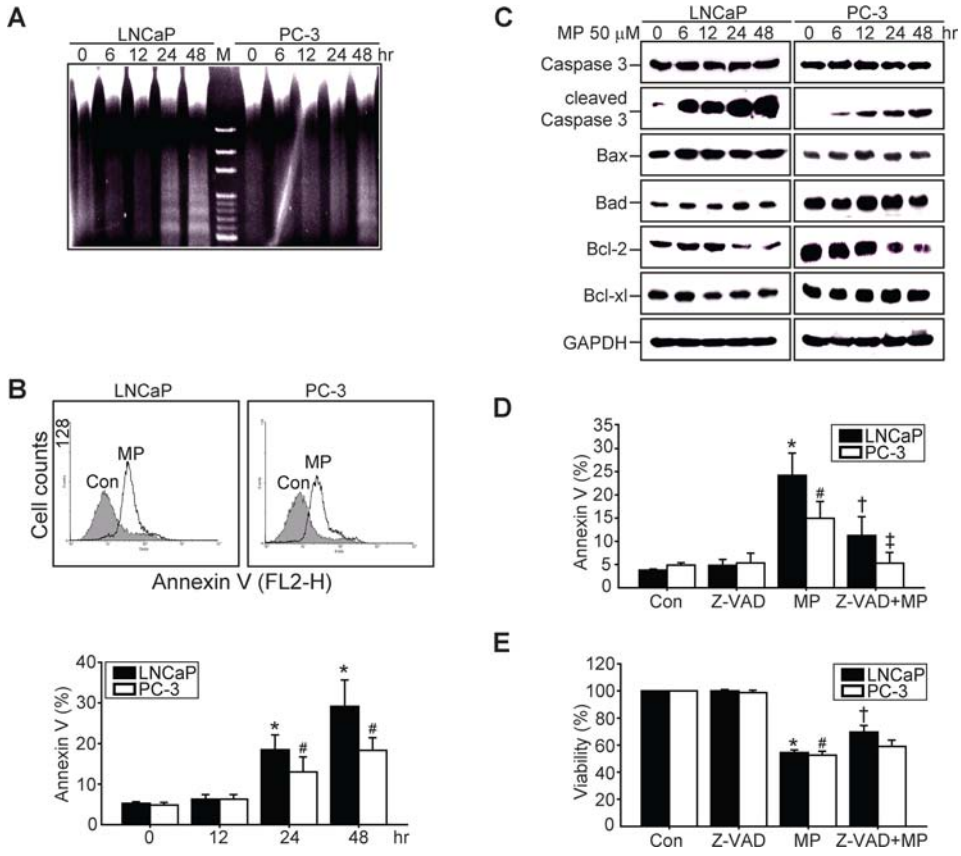

Figure 2. MP-induced apoptosis in prostate cancer cells. Apoptosis was assayed by (A) DNA laddering and (B) Annexin V staining, as determined using flow cytometry (top). Representative micrographs are shown (bottom). (∗) $p < 0.05$ compared to the LNCaP 0 h control. (#) $p < 0.05$ compared to the PC-3 0 h control. Mean ± SEM; $n = 3$. (C) Western blot analysis of caspase 3, cleaved caspase 3, Bax, Bad, Bcl-2, Bcl-xl, and GAPDH in both cells treated with 50 μM MP for the indicated times. LNCaP and PC-3 cells were pretreated with the pan-caspase inhibitor (Z-VAD) at a concentration of 20 μM for 1 h, followed by treatment with 50 μM MP for 48 h. Effects of Z-VAD on MP-induced apoptosis were evaluated by (D) Annexin V staining and (E) cell viability, as detected using the trypan blue exclusion assay. Mean ± SEM; $n = 3$. (∗) $p < 0.05$ compared to the LNCaP control. (#) $p < 0.05$ compared to the PC-3 control. (†) $p < 0.05$ compared to the LNCaP MP-treated group. (‡) $p < 0.05$ compared to the PC-3 MP-treated group.

significantly reverse in PC-3 cells pretreated with pan-caspase inhibitor (Figure 2E). We suggest the potential involvement of a different cell death pathway following MP treatment in PC-3 cells.

Monascuspiloin Induces Autophagic Cell Death in PC-3 Cells. We then determined whether MP induces autophagy in both cell lines. MP-induced autophagy in PC-3 cells was examined by the autophagic vacuoles containing cellular material using electron and fluorescence microscopy, respectively (panels A and B of Figure 3). Detection of increased levels of AVOs by flow cytometry as an indicator for autophagy induction demonstrated that MP treatment induced autophagy in approximately 35% of PC-3 cells after 48 h; in contrast, autophagy was observed in only 15% of LNCaP cells (Figure 3C). The hallmarks of autophagy, LC3-II, Atg5, and Beclin 1 expression, were also significantly induced in PC-3 cells following MP treatment (Figure 3D). Pretreated with the autophagy inhibitor 3-methyladenine (3-MA) significantly attenuates MP-induced autophagy and apoptosis, thereby reversed cell viability (Figure 3E) in PC-3 cells. The survival benefits achieved with 3-MA treatment indicate that MP treatment induces autophagy in PC-3 cells, resulting in apoptosis and cell death.

Apoptosis Induced by MP Treatment in LNCaP Cells Is Associated with the Inactivation of Akt/mTOR Signaling. We next evaluated the molecular mechanisms underlying MP-induced apoptosis and autophagy. The PI3K/Akt/mTOR pathways are key negative regulators of both apoptosis and autophagy. MP treatment decreased phosphorylation of Akt, mTOR, and p70S6K in both cell types (Figure 4A). The PI3K/Akt inhibitor Ly294002 (Ly) was used to determine the functional significance of Akt/mTOR/p70S6K activation in MP-induced apoptosis and autophagy. Treatment with Ly alone did not increase the basal level of apoptosis, but 2.5 μM Ly increased MP-induced apoptosis by approximately 30% in LNCaP cells, which suggests that MP treatment contributed to apoptosis in LNCaP cells by attenuating Akt activation (Figure 4B). However, Ly did not increase MP-induced autophagy (Figure 4C), suggesting that other signaling pathways may be responsible for autophagic cell death in PC-3 cells.

MP Treatment Induces Autophagic Cell Death in PC-3 Cells via Activation of AMPK Signaling. Molecular pathways accompanying the induction of apoptosis and autophagy also involve AMPK/TSC/mTOR signaling. Figure 4D shows that MP treatment resulting in significant phosphorylation of AMPK in a time-dependent manner. To test the role of AMPK in the induction of autophagy and apoptosis, PC-3 cells were transfected with AMPK-α1 shRNA (Figure 4E). AMPK-α1 shRNA-transfected cells were less sensitive to MP-induced apoptosis, autophagy, and cell death than control- and control-vector-transfected PC-3 cells (panels F and G of Figure 4). These results demonstrate that MP-induced autophagic and

dx.doi.org/10.1021/jf3016927 | J. Agric. Food Chem. 2012, 60, 7185−7193

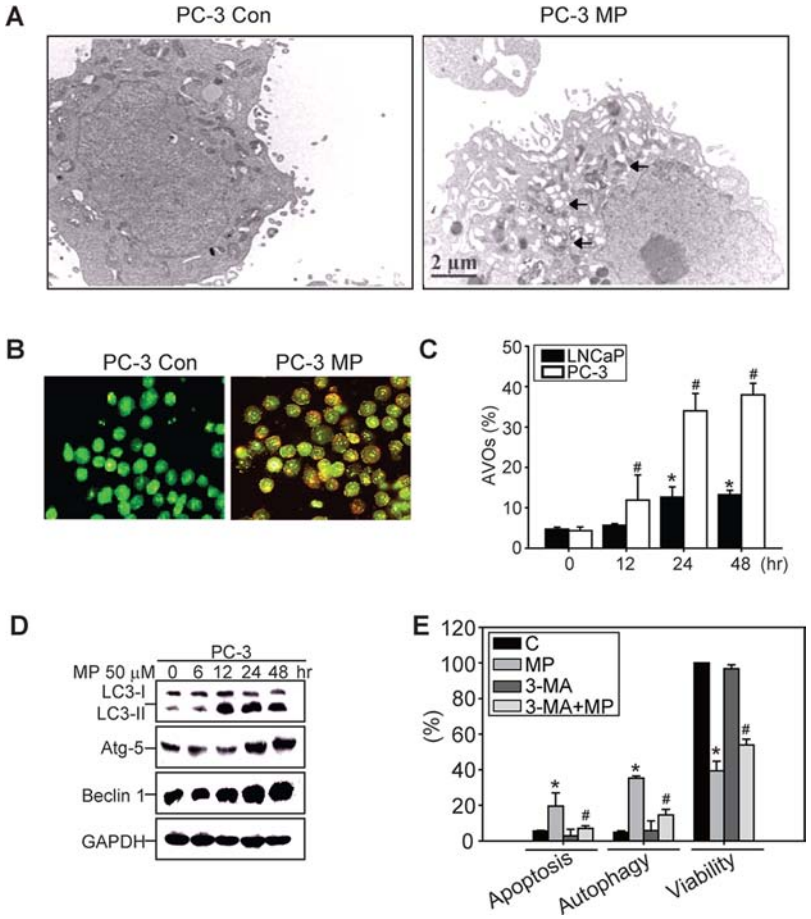

Figure 3. MP preferentially induces autophagy in androgen-independent PC-3 cells. (A) Representative electron microscopic images showing autophagic vacuoles (black arrows) in PC-3 cells treated with 50 μM MP for 48 h. (B) PC-3 cells treated with 50 μM MP for 48 h and then stained with AVOs. (C) Quantification of AVOs in AO-stained LNCaP and PC-3 cells treated with 50 μM MP for the indicated times using flow cytometry. Mean ± SEM; $n = 3$. (*) $p < 0.05$ compared to the LNCaP 0 h group. (#) $p < 0.05$ compared to the PC-3 0 h group. (D) Western blot analysis of LC3-I/II, Atg5, Beclin 1, and GAPDH in MP-treated PC-3 cells. (E) PC-3 cells were then pretreated with 2.5 mM 3-MA for 1 h followed by treatment with 50 μM MP for 48 h. Inhibition of apoptosis (stained with Annexin V) and autophagy (staining with AO) was determined using flow cytometry. Effects of 3-MA on MP-induced cell death were detected using the trypan blue exclusion assay. Mean ± SEM; $n = 3$. (*) $p < 0.05$ compared to the PC-3 control group. (#) $p < 0.05$ compared to the MP-treated group.

apoptotic cell death in PC-3 cells is dependent upon AMPK activation.

MP Treatment Inhibits PC-3 Xenograft Growth and Is Associated with Increased Apoptosis and Autophagy in Tumor Tissue. To evaluate whether MP could inhibit tumor growth *in vivo*, nude mice bearing PC-3 xenografts were treated with 40 or 120 mg/kg MP 3 times a week for 2 weeks. No appreciable toxicity, as assessed by a change in body weight, was detected following treatment with either dose (Figure 5A). As shown in panels B and C of Figure 5, MP significantly suppressed the growth of PC-3 tumors compared to the vehicle control group. On the 18th day after the first treatment, tumor growth was inhibited by ~63 and ~74% in the 40 and 120 mg/kg MP treatment groups, respectively (Table 1). Tumor volume quadrupling times (TVQTs) in the control, 40 mg/kg of MP, and 120 mg/kg of MP groups were approximately 18, 64, and 95 days, respectively (Table 1). Immunohistochemical staining demonstrated that the fraction of PCNA-positive cells was lower in the MP-treated groups. Moreover, the MP-treated groups exhibited slightly increased expression of cleaved caspase 3 but significantly induced Atg5 and LC3-II (Figure 5D). Western blot analysis confirmed that MP treatment induction slightly increased in apoptosis as detected by cleaved caspase 3 (Figure 5E) and induced autophagy as detected by the expression of cleaved LC3-II, Atg5, Atg12, and Beclin 1 (Figure 5E). These results demonstrate that the anticancer effects of MP treatment can be translated into animals and MP-mediated suppression of PC-3 xenograft growth was accompanied by apoptosis and autophagy. The present study demonstrated that MP exerts growth inhibitory effects on androgen-dependent and -independent prostate cancer cells *in vitro* and *in vivo*.

■ DISCUSSION

PCa is the most common malignant tumor in males worldwide. Advanced PCa is resistant to conventional therapies; thus, new compounds from natural resources and new strategies for PCa therapy are required.[23] Currently, natural products are receiving increased attention for the prevention and/or treatment of carcinogenesis because of their promising efficacy and low toxicity to normal tissues. One recent report indicated that a series of yellow pigments extracted from RMR were cytotoxic to cancer cells but not normal cells. Hence, *Monascus* pigments are now regarded as potential chemopreventive agents.[8] However, the molecular mechanisms of their anticancer properties remain largely unknown.

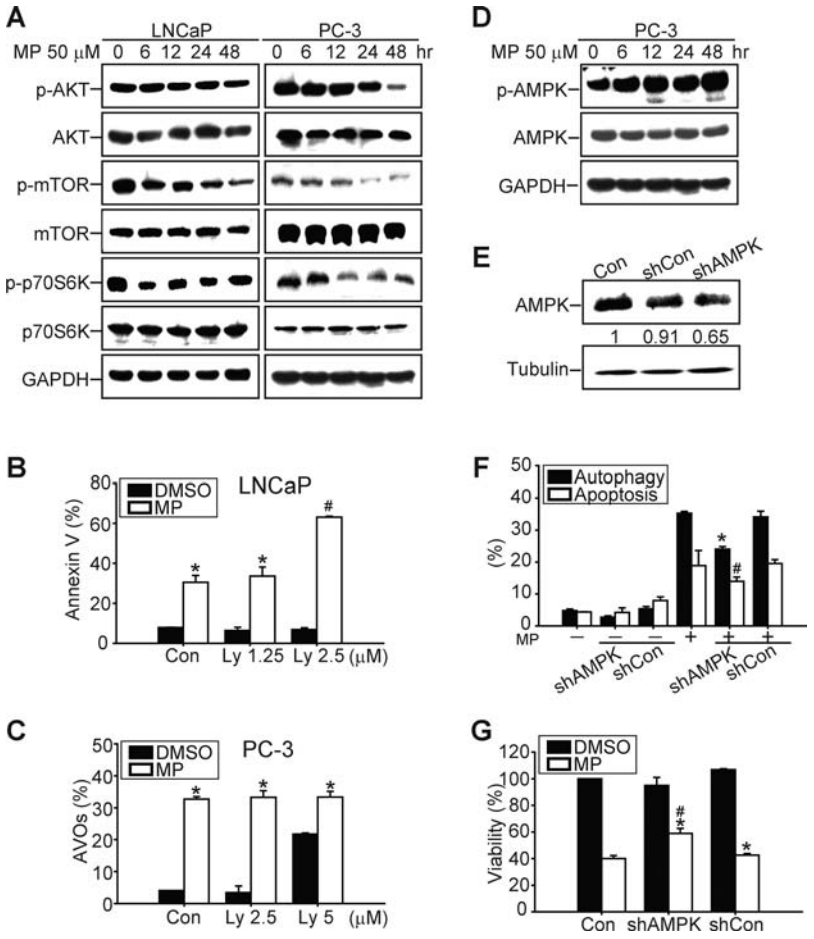

Figure 4. MP-induced apoptosis and autophagy is mediated by attenuating the PI3K/Akt signaling pathway and activating the AMPK signaling pathway. (A) Protein levels of pAkt, Akt, p-mTOR, mTOR, p-p70S6K, and p70S6K were analyzed by western blot using specific antibodies following treatment with 50 μM MP for the indicated times in LNCaP (left) and PC-3 (right) cells. (B) LNCaP cells were pretreated with 1.25 or 2.5 μM PI3K/Akt inhibitor Ly for 1 h, followed by 50 μM MP for 48 h. Apoptotic cells were quantified by Annexin V staining. Mean ± SEM; $n = 3$. (*) $p < 0.05$ compared to the control group. (#) $p < 0.05$ compared to the MP-treated alone. (C) AVOs were detected using flow cytometry of PC-3 cells pretreated with 2.5 or 5 μM Ly for 1 h followed by 50 μM MP for 48 h. Mean ± SEM; $n = 3$. (*) $p < 0.05$ compared to the control group. (D) Phosphorylation and expression of AMPK were determined using specific antibodies in PC-3 cells treated with 50 μM MP for 0, 6, 12, 24, and 48 h. (E) Western blot analysis of PC-3 cells transfected with 2 μg of control shRNA (shCon) or 2 μg of AMPK-α1 shRNA (shAMPK) for 48 h. The membrane was probed with anti-α-tubulin to confirm equal loading of the protein. The number below each line indicates the relative intensity of protein expression compared to the control (defined as 1). (F) Reduced apoptosis was measured by Annexin V staining. Autophagy was measured by AVOs. Mean ± SEM; $n = 3$. (*) $p < 0.05$ compared to the shCon MP-treated group. (#) $p < 0.05$ compared to the shCon MP-treated group. (G) Cell viability was determined using the trypan blue exclusion assay. Mean ± SEM; $n = 3$. (*) $p < 0.05$ compared to the dimethylsulfoxide (DMSO)-treated group. (#) $p < 0.05$ compared to the shCon MP-treated group.

Herein, we investigated the involvement of the PI3K/Akt/mTOR and AMPK pathways, two of the most important targets for prostate cancer therapy, in MP-induced apoptosis and autophagy. Recent studies have demonstrated that apoptosis can be negatively regulated by Akt through phosphorylation of Bad, Mcl-1, and Mdm2, which leads to inhibition of p53 transcriptional activity. Thus, inhibition of Akt could induce apoptosis in cancer cells, which makes it an attractive candidate for drug development.[24] Consistent with these observations, we found that phosphorylation of Akt and mTOR was inhibited by MP (Figure 4A). Inhibition of Akt activity by PI3K/Akt inhibitor further increased the apoptotic index in MP-treated LNCaP cells. In contrast, treatment of PC-3 cells with PI3K/Akt inhibitor alone increased autophagy but did not further enhance autophagy in the MP-treated PC-3 cells (Figure 4C). These results suggest that the Akt/mTOR pathway contributes to apoptosis in LNCaP cells; however, there is no direct relationship between the Akt/mTOR pathway and autophagy in PC-3 cells following MP treatment. Similar to our results, Hu et al. reported that Akt levels are not a key determinant of autophagy induction by penta-1,2,3,4,6-*O*-galloyl-β-D-glucose (PGG) in PC-3 cells.[25] Additionally, upregulation of Akt can also promote cell growth by inactivating the negative cell cycle regulators p21 and p27.[26] Thus, we hypothesized that inhibition of Akt by MP in PC-3 cells may preferentially contribute to G2/M arrest but not autophagy.

We then hypothesized that MP inhibits mTOR through a different signaling pathway to induce autophagy. AMPK is a master regulator of lipogenic pathways, and activation of AMPK leads to mTOR inhibition and induction of autophagy. A previous report indicated that AMPK activators could inhibit 90% of the cell growth of androgen-independent DU145 and PC-3 cells. This inhibition was associated with increased expression of the cell cycle inhibitor p21, inhibition of mTOR signaling, and decreased concentrations of malonyl CoA, an

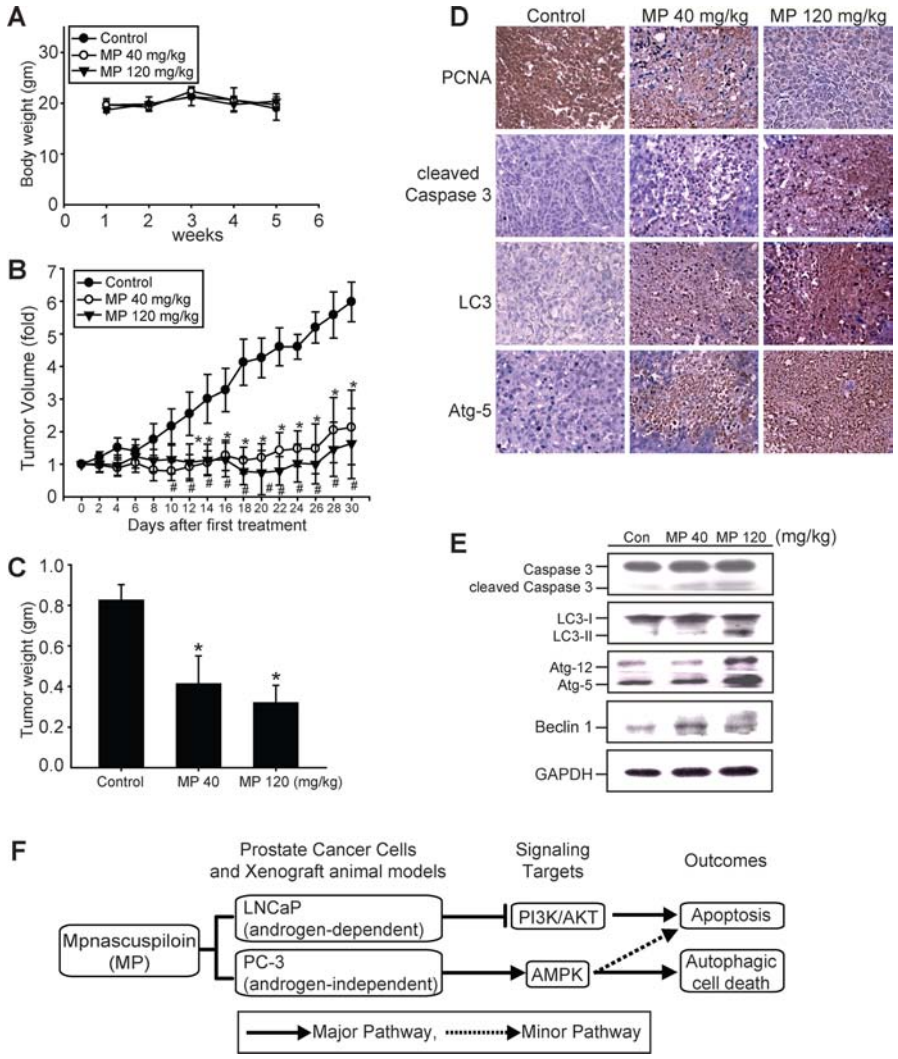

Figure 5. MP inhibited PC-3 xenograft growth and was associated with increased apoptosis and autophagy of the tumor cells. PC-3-bearing nude mice were administered 40 or 120 mg/kg of MP or corn oil (control) alone intraperitoneally 3 times a week for 2 weeks. (A) Body weight was measured in nude mice once a week. (B) Tumor volume was measured once every 2 days. Data are presented as the relative tumor volume normalized to the initial tumor volume measured on day 0. After sacrifice, (C) tumor weights in control mice and MP-treated mice were measured. (∗) $p < 0.05$ compared to the control group. (D) Tumors were removed and stained with PCNA, cleaved caspase 3, LC3, and Atg5 by immunohistochemistry. (E) Immunoblotting for cleaved caspase 3, LC3-II, Atg12, Atg5, and Beclin 1 using tumor supernatants from control and MP-treated groups. (F) Proposed mechanism by which MP treatment induces cell death in prostate cancer cells. MP preferentially induced apoptosis in LNCaP cells through inhibition of PI3K/Akt signaling, whereas it induced autophagic cell death in PC-3 cells via activation of AMPK signaling.

Table 1. Comparison of Tumor Growth Inhibition, Tumor Volume Quadrupling Time, and Tumor Growth Delay Time of PC-3 Tumors in Nude Mice Treated with Corn Oil (Control), 40 and 120 mg/kg of MP[a]

	number of mice	inhibition (%)[c]	tumor volume quadruping time (day)	tumor growth delay time (day)	p value (t test)[b]	
					control	40 mg
control	5		17.9 ± 2.2			
40 mg	5	63.0 ± 12.3	63.68 ± 7.4	45.8 ± 7.4	0.08	
120 mg	5	74.3 ± 13.44	94.51 ± 8.1	76.61 ± 8.1	<0.05	0.64

[a]Mean ± SEM; $n = 5$. [b]$p < 0.05$; significance estimated by the Student's t test in comparison to the tumor growth delay time of the control group. [c]$p < 0.05$ compared to the control group on day 18.

intermediate of *de novo* fatty acid synthesis.[27] Johnson et al. reported that carnosol, a dietary diterpene isolated from culinary herbs, inhibited the PI3K/Akt pathway and activated the AMPK pathway, leading to mTOR inhibition and G2 cell cycle arrest.[28] One recent report also demonstrated that geraniol can inhibit Akt and activate AMPK, which results in mTOR inhibition in PC-3 cells.[29] Thus, the use of AMPK activators may represent a promising therapeutic strategy for PCa by inducing cell cycle arrest and autophagy. Consistent with these reports, our results demonstrate that shRNA-mediated inhibition of AMPK reduced autophagy and apoptosis and, consequently, increased the viability of MP-treated PC-3 cells (panels E–G of Figure 4). We found that MP-activated AMPK contributes to autophagy, thereby

inducing apoptosis in PC-3 cells. Thus, MP could likely be used as a potential cancer therapeutic agent through targeting both the Akt and AMPK pathways in PCa.

Autophagy can promote the survival of normal cells during nutrient starvation, and similarly, autophagy may buffer metabolic stress and enhance the survival of cancer cells. Nevertheless, autophagy could also serve as a pro-death mechanism in cancer cells.[30] A series of studies have indicated that autophagy can lead to cell death in apoptosis-defective tumor cells that are triggered by nutrient and growth factor deprivation, radiation stimuli, or chemotherapy. For example, fisetin has been reported to induce autophagic cell death in hormone-refractory PC-3 cells through suppression of the mTOR pathway.[31] Penta-1,2,3,4,6-*O*-galloyl-*β*-D-glucose has also been shown to induce autophagy and caspase-independent programmed cell death in PC-3 cells.[25] Using autophagy inhibitor 3-MA, we currently found that inhibition of autophagy could reduce apoptosis and reverse cell viability in MP-treated PC-3 cells, suggesting that MP-induced autophagy triggers a pro-death response. Therefore, MP-induced autophagy in PC-3 cells may act as an alternative to the dominant cell death pathway, and targeting autophagic signaling pathways could potentially result in novel prostate cancer therapies.

The induction of both autophagy and apoptosis by MP prompted us to investigate the interconnection between these two cellular processes. The induction of autophagy in PC-3 cells promoted apoptosis and indicated that autophagy contributes to apoptosis (Figure 4). In this respect, autophagy seems to facilitate apoptosis in PC-3 cells. This notion is supported by the observation that inhibition of autophagy by 3-MA or AMPK shRNA decreased cell sensitivity to MP-induced apoptosis (Figures 3E and 4F). Consistent with these data, previous reports have indicated that autophagy can function upstream of apoptosis by different mechanisms. For example, autophagy is reported to maintain cellular ATP levels, which leads to apoptosis in response to stimuli.[32] Thus, our results highlight that the important significance of MP-induced autophagy can not only kill cancer cells but also sensitize androgen-independent PC-3 cells to apoptosis. Nevertheless, molecular mechanisms governing the role of autophagy in MP-induced apoptosis required further study.

Direct evidence to support the *in vitro* antitumor activity of MP was provided by our *in vivo* PC-3 xenograft model in SCID mice. Tumor growth was suppressed following MP treatment, resulting in a significant difference in tumor volume and tumor weight and a delay in tumor growth compared to untreated control tumors (Figure 5 and Table 1). MP-induced cytotoxicity is complex and related to several different cell death pathways. Our current *in vivo* results indicate that expression levels of LC3-II, Atg5, Beclin 1, and cleaved caspase 3 proteins were increased following MP treatment; in contrast, PCNA expression was decreased in the PC-3 mouse xenograft model (Figure 5D). These findings suggest that the MP-induced antitumor growth effect *in vivo* was a result of the induction of autophagy and apoptosis in prostate cancer cells. Additionally, the lack of toxicity is important when evaluating the potential value of a chemopreventive agent. The fact that MP attenuated the xenograft growth without inducing significant toxicity, as measured by body weight loss (Figure 5A), indicates that MP is safe for further preclinical testing in PCa.

Taken together, our study provides evidence that MP, a novel monascin analogue, could suppress the growth of both androgen-dependent and -independent prostate cancer cells through different mechanisms (Figure 5F). Specifically, MP preferentially induces apoptosis in androgen-dependent LNCaP cells through inhibition of the PI3K/Akt/mTOR pathways, whereas MP induces autophagic cell death in hormone-refractory PC-3 cells through AMPK-dependent pathways. Induction of autophagy in PC-3 cells further sensitizes cells to apoptosis induced by MP. Additionally, MP also induces G2/M arrest in PC-3 cells with a concomitant accumulation of cyclin B and phospho-Cdc2 (Y15). To our knowledge, this study is the first to demonstrate that MP induces autophagy and apoptosis in prostate cancer cells through the PI3K/Akt and AMPK signaling pathways. We conclude that MP is a potential cancer therapeutic agent and is worthy of further study. Administration of MP to inhibit Akt and activate AMPK signaling could represent novel therapeutic strategies for the treatment of human prostate cancer.

AUTHOR INFORMATION

Corresponding Author

*Telephone: 886-6-235-3535, ext. 5804. Fax: 886-6-275-2484. E-mail: yjwang@mail.ncku.edu.tw.

Funding

We thank the commission of this study by the Food Industry Research and Development Institute and the financial support (99-EC-17-A-01-04-0525) of the Ministry of Economic Affairs, the Republic of China. We also thank the National Science Council (NSC 100-2314-B-006-055) and Food and Drug Administration, Department of Health, Executive Yuan (DOH101-FDA-41301) for their support.

Notes

The authors declare no competing financial interest.

REFERENCES

(1) Knecht, A.; Humpf, H. U. Cytotoxic and antimitotic effects of N-containing *Monascus* metabolites studied using immortalized human kidney epithelial cells. *Mol. Nutr. Food Res.* **2006**, *50*, 406−412.

(2) Lin, Y. L.; Wang, T. H.; Lee, M. H.; Su, N. W. Biologically active components and nutraceuticals in the *Monascus*-fermented rice: A review. *Appl. Microbiol. Biotechnol.* **2008**, *77*, 965−973.

(3) Cheng, M. J.; Wu, M. D.; Chen, I. S.; Yuan, G. F. A new sesquiterpene isolated from the extracts of the fungus *Monascus pilosus*-fermented rice. *Nat. Prod. Res.* **2010**, *24*, 750−758.

(4) Su, Y. C.; Wang, J. J.; Lin, T. T.; Pan, T. M. Production of the secondary metabolites γ-aminobutyric acid and monacolin K by *Monascus*. *J. Ind. Microbiol. Biotechnol.* **2003**, *30*, 41−46.

(5) Taira, J.; Miyagi, C.; Aniya, Y. Dimerumic acid as an antioxidant from the mold, *Monascus anka*: The inhibition mechanisms against lipid peroxidation and hemeprotein-mediated oxidation. *Biochem. Pharmacol.* **2002**, *63*, 1019−1026.

(6) Blanc, P. J.; Laussac, J. P.; Le Bars, J.; Le Bars, P.; Loret, M. O.; Pareilleux, A.; Prome, D.; Prome, J. C.; Santerre, A. L.; Goma, G. Characterization of monascidin A from *Monascus* as citrinin. *Int. J. Food Microbiol.* **1995**, *27*, 201−213.

(7) Zheng, Y.; Xin, Y.; Shi, X.; Guo, Y. Cytotoxicity of *Monascus* pigments and their derivatives to human cancer cells. *J. Agric. Food Chem.* **2010**, *58*, 9523−9528.

(8) Hong, M. Y.; Henning, S.; Moro, A.; Seeram, N. P.; Zhang, Y.; Heber, D. Chinese red yeast rice inhibition of prostate tumor growth in SCID mice. *Cancer Prev. Res.* **2011**, *4*, 608−615.

(9) Kim, C.; Jung, H.; Kim, Y. O.; Shin, C. S. Antimicrobial activities of amino acid derivatives of *Monascus* pigments. *FEMS Microbiol. Lett.* **2006**, *264*, 117−124.

(10) Yasukawa, K.; Takahashi, M.; Natori, S.; Kawai, K.; Yamazaki, M.; Takeuchi, M.; Takido, M. Azaphilones inhibit tumor promotion by

12-*O*-tetradecanoylphorbol-13-acetate in two-stage carcinogenesis in mice. *Oncology* **1994**, *51*, 108−112.
(11) Akihisa, T.; Tokuda, H.; Yasukawa, K.; Ukiya, M.; Kiyota, A.; Sakamoto, N.; Suzuki, T.; Tanabe, N.; Nishino, H. Azaphilones, furanoisophthalides, and amino acids from the extracts of *Monascus pilosus*-fermented rice (red-mold rice) and their chemopreventive effects. *J. Agric. Food Chem.* **2005**, *53*, 562−565.
(12) Li, J. J.; Shang, X. Y.; Li, L. L.; Liu, M. T.; Zheng, J. Q.; Jin, Z. L. New cytotoxic azaphilones from *Monascus purpureus*-fermented rice (red yeast rice). *Molecules* **2010**, *15*, 1958−1966.
(13) Hsu, Y. W.; Hsu, L. C.; Liang, Y. H.; Kuo, Y. H.; Pan, T. M. Monaphilones A−C, three new antiproliferative azaphilone derivatives from *Monascus purpureus* NTU 568. *J. Agric. Food Chem.* **2010**, *58*, 8211−8216.
(14) Hong, M. Y.; Seeram, N. P.; Zhang, Y.; Heber, D. Chinese red yeast rice versus lovastatin effects on prostate cancer cells with and without androgen receptor overexpression. *J. Med. Food* **2008**, *11*, 657−666.
(15) Shen, M. M.; Abate-Shen, C. Molecular genetics of prostate cancer: New prospects for old challenges. *Genes Dev.* **2010**, *24*, 1967−2000.
(16) Jemal, A.; Siegel, R.; Ward, E.; Hao, Y.; Xu, J.; Murray, T.; Thun, M. J. Cancer statistics, 2008. *Ca-Cancer J. Clin.* **2008**, *58*, 71−96.
(17) Sarker, D.; Reid, A. H.; Yap, T. A.; de Bono, J. S. Targeting the PI3K/AKT pathway for the treatment of prostate cancer. *Clin. Cancer Res.* **2009**, *15*, 4799−4805.
(18) Hardie, D. G. AMP-activated/SNF1 protein kinases: Conserved guardians of cellular energy. *Nat. Rev. Mol. Cell Biol.* **2007**, *8*, 774−785.
(19) Flavin, R.; Zadra, G.; Loda, M. Metabolic alterations and targeted therapies in prostate cancer. *J. Pathol.* **2011**, *223*, 283−294.
(20) Crighton, D.; Wilkinson, S.; O'Prey, J.; Syed, N.; Smith, P.; Harrison, P. R.; Gasco, M.; Garrone, O.; Crook, T.; Ryan, K. M. DRAM, a p53-induced modulator of autophagy, is critical for apoptosis. *Cell* **2006**, *126*, 121−134.
(21) Dalby, K. N.; Tekedereli, I.; Lopez-Berestein, G.; Ozpolat, B. Targeting the prodeath and prosurvival functions of autophagy as novel therapeutic strategies in cancer. *Autophagy* **2010**, *6*, 322−329.
(22) Chen, R. J.; Ho, C. T.; Wang, Y. J. Pterostilbene induces autophagy and apoptosis in sensitive and chemoresistant human bladder cancer cells. *Mol. Nutr. Food Res.* **2010**, *54*, 1819−1832.
(23) Wang, L. G.; Chiao, J. W. Prostate cancer chemopreventive activity of phenethyl isothiocyanate through epigenetic regulation (review). *Int. J. Oncol.* **2010**, *37*, 533−539.
(24) Majumder, P. K.; Sellers, W. R. Akt-regulated pathways in prostate cancer. *Oncogene* **2005**, *24*, 7465−7474.
(25) Hu, H.; Chai, Y.; Wang, L.; Zhang, J.; Lee, H. J.; Kim, S. H.; Lu, J. Pentagalloylglucose induces autophagy and caspase-independent programmed deaths in human PC-3 and mouse TRAMP-C2 prostate cancer cells. *Mol. Cancer Ther.* **2009**, *8*, 2833−2843.
(26) Gao, D.; Inuzuka, H.; Tseng, A.; Wei, W. Akt finds its new path to regulate cell cycle through modulating Skp2 activity and its destruction by APC/Cdh1. *Cell Div.* **2009**, *4*, 11.
(27) Xiang, X.; Saha, A. K.; Wen, R.; Ruderman, N. B.; Luo, Z. AMP-activated protein kinase activators can inhibit the growth of prostate cancer cells by multiple mechanisms. *Biochem. Biophys. Res. Commun.* **2004**, *321*, 161−167.
(28) Johnson, J. J.; Syed, D. N.; Heren, C. R.; Suh, Y.; Adhami, V. M.; Mukhtar, H. Carnosol, a dietary diterpene, displays growth inhibitory effects in human prostate cancer PC3 cells leading to G2-phase cell cycle arrest and targets the 5′-AMP-activated protein kinase (AMPK) pathway. *Pharm. Res.* **2008**, *25*, 2125−2134.
(29) Kim, S. H.; Park, E. J.; Lee, C. R.; Chun, J. N.; Cho, N. H.; Kim, I. G.; Lee, S.; Kim, T. W.; Park, H. H.; So, I.; Jeon, J. H. Geraniol induces cooperative interaction of apoptosis and autophagy to elicit cell death in PC-3 prostate cancer cells. *Int. J. Oncol.* **2011**, *5*, 1683−1718.
(30) Gozuacik, D.; Kimchi, A. Autophagy as a cell death and tumor suppressor mechanism. *Oncogene* **2004**, *23*, 2891−2906.
(31) Sun, Y. W.; Huang, W. J.; Hsiao, C. J.; Chen, Y. C.; Lu, P. H.; Guh, J. H. Methoxychalcone induces cell-cycle arrest and apoptosis in human hormone-resistant prostate cancer cells through PI 3-kinase-independent inhibition of mTOR pathways. *Prostate* **2010**, *70*, 1295−1306.
(32) Yoshimori, T. Autophagy: Paying Charon's toll. *Cell* **2007**, *128*, 833−836.